

## FEATURED ARTICLE

# Contribution of Alzheimer's disease pathology to biological and clinical progression: A longitudinal study across two cohorts

Wei Zhang<sup>1,2</sup> | Hui-Fu Wang<sup>1,3</sup> | Kevin Kuo<sup>1</sup> | Linbo Wang<sup>1,2</sup> | Yuzhu Li<sup>1,2</sup> |  
Jintai Yu<sup>1</sup> | Jianfeng Feng<sup>1,2,4,5,6,7</sup> | Wei Cheng<sup>1,2,4,8</sup>

<sup>1</sup>Institute of Science and Technology for Brain-Inspired Intelligence, and Department of Neurology, Huashan Hospital, Fudan University, Shanghai, China

<sup>2</sup>Key Laboratory of Computational Neuroscience and Brain Inspired Intelligence (Fudan University), Ministry of Education, Shanghai, China

<sup>3</sup>Department of Neurology, Qingdao Municipal Hospital, Qingdao University, Qingdao, China

<sup>4</sup>Fudan ISTBI–ZJNU Algorithm Centre for Brain-Inspired Intelligence, Zhejiang Normal University, Jinhua, China

<sup>5</sup>Zhangjiang Fudan International Innovation Center, Shanghai, China

<sup>6</sup>Department of Computer Science, University of Warwick, Coventry, UK

<sup>7</sup>School of Data Science, Fudan University, Shanghai, China

<sup>8</sup>Shanghai Medical College and Zhongshan Hospital Immunotherapy Technology Transfer Center, Fudan University, Shanghai, China

## Correspondence

Wei Cheng, Institute of Science and Technology for Brain-Inspired Intelligence, Fudan University, Shanghai, China.  
E-mail: [wcheng@fudan.edu.cn](mailto:wcheng@fudan.edu.cn)

## Funding information

National Natural Science Foundation of China, Grant/Award Numbers: 82071997, 82071201; National Key R&D Program of China, Grant/Award Numbers: 2019YFA0709502, 2018YFC1312904; Shanghai Municipal Science and Technology Major Project, Grant/Award Number: 2018SHZDZX01; 111 Project, Grant/Award Number: B18015; Science and Technology Innovation 2030 Major Projects, Grant/Award Number: 2022ZD0211600; Shanghai Rising-Star Program, Grant/Award Number: 21QA1408700; Shanghai Municipal Health Commission New interdisciplinary research project, Grant/Award Number: 2022JC014; STI2030-Major Projects, Grant/Award Number: 2022ZD0211600; Taishan Scholars Program of Shandong Province, Grant/Award Number: tsqn201812157

## Abstract

**INTRODUCTION:** Amyloid beta ( $A\beta$ ) deposition, tau accumulation, and brain atrophy occur in sequence, but the contribution of Alzheimer's disease (AD) pathology to biological and clinical progression remains unclear.

**METHODS:** We included 290 and 70 participants with longitudinal assessment on  $A\beta$ -positron emission tomography (PET), tau-PET, magnetic resonance imaging, and cognitive function from the Harvard Aging Brain Study (HABS) and Alzheimer's Disease Neuroimaging Initiative (ADNI) datasets, respectively. Partial least squares structural equation modeling (PLS-SEM) was used to determine the contribution of AD pathology to the biological and clinical longitudinal changes.

**RESULTS:** Imaging biomarkers and cognitive function were significantly associated in cross-sectional and longitudinal analyses. At the final time point, the percentage of variance explained by PLS-SEM was 27% for  $A\beta$ , 30% for tau ( $A\beta$  accounted for 61%), 29% for brain atrophy (tau accounted for 37%), and 37% for cognitive decline (brain atrophy accounted for 35%).

**DISCUSSION:** This study highlights distinctive contributing proportions of AD pathology to biological and clinical progression. Treatments targeting  $A\beta$  and tau may partially block AD progression.

## KEYWORDS

Alzheimer's disease, amyloid beta, cognitive decline, magnetic resonance imaging, positron emission tomography, quantification, tau protein

Wei Zhang and Hui-Fu Wang contributed equally to this study.

## 1 | BACKGROUND

Alzheimer's disease (AD) is a neurodegenerative disorder characterized by a triad of neuropathological hallmarks, including amyloid beta ( $A\beta$ ) plaques, tau neurofibrillary tangles, and neurodegeneration.<sup>1</sup> The prevailing hypothesis has posited an instigating role of  $A\beta$ , in which the  $A\beta$  deposition could incite a cascade for tau propagation and neuritic alterations that subsequently lead to AD progression.<sup>1,2</sup> The National Institute on Aging–Alzheimer's Association (NIA-AA) has previously proposed a biomarker-based framework which explicitly defines the mechanistic context of AD that reconciles the hypothesis.<sup>3</sup> Accordingly, the NIA-AA framework consists of three biomarkers: A—multimerized  $A\beta$  (lower  $A\beta$  level in cerebrospinal fluid [CSF] or  $A\beta$  deposition on positron emission tomography [PET]); T—multimerized tau (higher phosphorylated tau [p-tau] level in CSF or tau accumulation on PET); and N—neurodegeneration (e.g., high total tau [t-tau] level in CSF or brain atrophy on magnetic resonance imaging [MRI]).<sup>3,4</sup> Since its release, the NIA-AA research framework has brought tremendous advancement to the standardized characterization of AD.

However, this framework has made no a priori assumptions regarding the relative pathogenicity of different biomarkers, and thus the extent to which AD pathology accounts for disease progression and clinical symptoms has remained ambiguous. Unraveling the contributions of AD pathology, especially the precise pathological sequence and effects among each biomarker, is critical to improving the diagnostic framework and therapeutic approaches. Previous investigations have provided support to the distinctive contributing proportion of AD pathology. For instance, an earlier study has suggested the existence of neuropathologic heterogeneity in AD, where it has shown a substantial contributing proportion of AD pathology to cognitive loss in the elderly,<sup>5</sup> ranging from 22% to 100% at the individual level. More recently, a multimodal study has identified that  $A\beta$ , tau, and cortical atrophy accounted for 16%, 46% to 47%, and 25% to 29%, respectively, of the variance in cognitive decline. Still, these findings have only captured partial aspects, as they have failed to address the longitudinal changes of biomarkers and their potential contributions to each other.

In addition, because  $A\beta$  plaques are the key pathology for AD and emerge at least a decade before the onset of clinical symptoms,<sup>2,6</sup> clinical trials were designed to test the efficacy of the treatments targeting  $A\beta$  in AD patients.<sup>7</sup> However, these treatments did not significantly prevent cognitive decline in almost all clinical trials except aducanumab being reported to be effective previously.<sup>8–11</sup> Several explanations were proposed for the therapeutic failure: that the intervention was administered too late in the entire course, that  $A\beta$  was not the optimal target even if  $A\beta$  deposition occurred first in the disease progression, and that not all the biological and clinical progression in AD continuum resulted from AD pathology.<sup>12,13</sup> These interpretations emphasized the complexity of AD pathological progression and cognitive decline, and indicated that it was necessary to verify the precise temporal sequence and the accurate effects of pathological markers on disease progression for developing effective treatments for AD.

### RESEARCH IN CONTEXT

- 1. Systematic Review:** The prevailing hypothesis posits that amyloid beta ( $A\beta$ ) deposition incites tau accumulation and subsequently leads to brain atrophy and cognitive decline in Alzheimer's disease (AD) progression. However, the contribution of prior AD pathology to the subsequent biological and clinical progression remained undetermined.
- 2. Interpretation:** Imaging biomarkers and cognitive function were significantly associated in cross-sectional and longitudinal analyses. At the final time point, the percentage of variance explained by integrating AD pathology and risk factors was 27% for  $A\beta$  deposition, 30% for tau accumulation, 29% for brain atrophy, and 37% for cognitive decline. Further,  $A\beta$  burden accounted for 61% of explained variance in tau accumulation, tau accumulation accounted for 37% of explained variance in cortical thickness, and cortical thickness accounted for 35% of explained variance in cognitive decline.
- 3. Future Directions:** Investigation of the role of treatments targeting  $A\beta$  and tau in alleviating the process of neurodegeneration and cognitive decline is needed in clinical trials.

By leveraging multimodal neuroimaging data derived from the Harvard Aging Brain Study (HABS) and Alzheimer's Disease Neuroimaging Initiative (ADNI), our objective is to quantify contributing proportions of  $A\beta$ , tau, and brain atrophy to biological and clinical progression throughout the disease continuum.

## 2 | METHODS

### 2.1 | Primary dataset: the HABS dataset

The HABS is a longitudinal observational study of aging and pre-clinical stages of AD.<sup>14</sup> The HABS protocol was approved by the Partners Institutional Review Board. All participants provided written informed consent upon recruitment. HABS 2.0 data release was used in this investigation, which includes 290 participants with up to 5-year follow-ups. The data used in this study contained  $A\beta$ -PET, tau-PET, T1-weighted structural MRI (sMRI), and cognitive measures. Longitudinal data were acquired for  $A\beta$ -PET, sMRI, and cognition from 2010. The initial tau-PET collected in 2013 was defined as baseline ( $t = 0$ , where  $t$  indicates the time in years from baseline) because the tau-PET was collected since 2013, and the term initial tau-PET is equivalent to baseline tau-PET. The initial time of  $A\beta$ -PET, sMRI, and cognition was  $t = -3$ . The final collections of these data were performed at  $t = 2$ .

## 2.2 | Cross-validation dataset: the ADNI dataset

The ADNI dataset was used for replication and validation.<sup>15</sup> The study was approved by the institutional review boards of all participating centers, and written informed consent was obtained from all participants or authorized representatives. The inclusion criteria were as follows. All subjects had to complete A $\beta$ -PET, tau-PET, T1-weighted sMRI, and cognitive measures at baseline and 2-year follow-up visit; the collection time of each modality should not differ by more than 3 months. The selection procedures resulted in a total of 70 study samples from ADNI. The data were accessed on May 20, 2022, and the detailed descriptions of the two datasets can be found in the [supplementary materials](#) in supporting information.

## 2.3 | Cognitive measures

Participants in HABS are evaluated annually with a battery of cognitive assessments. The Preclinical Alzheimer's Cognitive Composite + Semantic Fluency (PACC5) was used as the measure of cognitive change over time, and this composite was developed to be sensitive to early cognitive changes in AD.<sup>16,17</sup> A modified version of PACC5 was used as the cognitive outcome measure in the ADNI dataset.<sup>18</sup> Higher PACC5 scores reflect better performance. The detailed description and calculation of cognitive assessments are in the [supplementary materials](#).

## 2.4 | Structural MRI data

Structural MRI data in HABS were acquired at years 1 (time = -3), year 4 (time = 0), and year 6 (time = 2). FreeSurfer v6.0 was used to preprocess the sMRI images.<sup>19</sup> The Desikan-Killiany atlas corresponding to 68 regions of interest (ROIs) was used to estimate the mean cortical thickness. The description of acquisition protocols and imaging preprocessing can be found in the [supplementary materials](#).

## 2.5 | PET imaging

In HABS, fibrillar A $\beta$  deposition was assessed using C-11 Pittsburgh compound B (PiB), and tau burden was measured using F-18 flortaucipir (AV1451). The ADNI uses the F-18 florbetapir (AV45) as the A $\beta$ -PET tracer and the F-18 flortaucipir (AV1451) as the tau-PET tracer. The details of PET imaging can be found in the [supplementary materials](#).

PET data were preprocessed using PETSURFER in FreeSurfer.<sup>20,21</sup> Taking cerebellar gray matter as the reference region, the mean standardized uptake value ratio (SUVR) of each brain region was calculated based on the Desikan-Killiany atlas. Partial volume correction was applied for PET data using the geometric transfer matrix method.<sup>22</sup>

## 2.6 | Statistical analysis

Linear mixed models were used to estimate the change rates of A $\beta$ , tau, and cortical thickness in each brain region over time and were implemented in MATLAB 2018b using the fitlme function. All models included baseline age, sex, race, years of education, apolipoprotein E (APOE)  $\epsilon$ 4 status (carrier or non-carrier), and time (entire follow-up) as fixed effects. Individual intercepts and slopes were modeled as random effects. Statistical significance was established as two-tailed  $P < 0.05$  after Benjamini-Hochberg false discovery rate (FDR) correction.<sup>23</sup> The brain regions with significant change rates were selected as meta-ROI for A $\beta$ , tau, and cortical thickness. For each participant, the summary value of every imaging modality at different time points was calculated separately, based on the corresponding meta-ROI. The linear mixed models with random intercept and time slope were used to estimate the individual change rates of cognition and the summary value of A $\beta$ , tau, and cortical thickness.

The relationships among AD imaging biomarkers (A $\beta$  deposition, tau burden, and cortical thickness from all ROIs), cognition, and AD risk factors (age, sex, years of education, and APOE  $\epsilon$ 4 status) were assessed using partial least squares structural equation modeling (PLS-SEM, implemented in "plsrm" R package),<sup>24</sup> testing an a priori hypothesized A $\beta$ -tau-atrophy-cognition pathway following the sequence of baseline, slope, final time point (see illustration in Figure 3A). The results were corrected using FDR ( $P < 0.05$ ). Details of model fitting and evaluation can be found in the [supplementary materials](#). In addition, a fully connected model was also fitted, which could freely estimate other possible orders, and the results are presented in the [supplementary materials](#).

## 3 | RESULTS

### 3.1 | Demographics

The sample used in these analyses included 290 participants from HABS and 70 participants from ADNI (Table 1). There were no significant differences between the two cohorts in the proportion of sex ( $\chi^2 = 0.038$ ,  $P = 0.845$ ) and APOE  $\epsilon$ 4 carrier ( $\chi^2 = 2.292$ ,  $P = 0.130$ ). However, compared to ADNI, participants in HABS were younger ( $t = 3.545$ ,  $P < 0.001$ ) and had fewer years of education ( $t = -2.541$ ,  $P = 0.011$ ).

### 3.2 | The longitudinal changes of A $\beta$ , tau, and cortical thickness

Spatiotemporal progression of A $\beta$ , tau, and cortical thickness are listed in Figure 1 (FDR corrected,  $P < 0.05$ ). A $\beta$  accumulated significantly in 65 brain regions, in which more rapid accumulations were identified in the rostral anterior cingulate, middle frontal gyrus, and precuneus regions. Unlike A $\beta$  deposition across the cortex, tau accumulation appeared to be localized, especially in the inferior, middle,

**TABLE 1** Demographics characteristics of the participants in the HABS and ADNI dataset.

Characteristics	Primary dataset: HABS	Cross-validation dataset: ADNI	P-value
N	290	70	–
Age at inclusion, year	73.7 (6.2)	70.8 (6.5)	<0.001
Female, %	59.3%	57.1%	0.845
Education, year	15.8 (3.1)	16.8 (2.3)	0.011
APOE $\epsilon$ 4 carriers, %	27.2% (missing = 3)	37.1% (missing = 1)	0.130
PACC slope	–0.039 (0.101)	–0.076 (0.082)	<0.001

Note: Values are presented as mean (standard deviation).

Abbreviations: ADNI, Alzheimer's Disease Neuroimaging Initiative; APOE, apolipoprotein E; HABS, Harvard Aging Brain Study; PACC, Preclinical Alzheimer's Cognitive Composite.

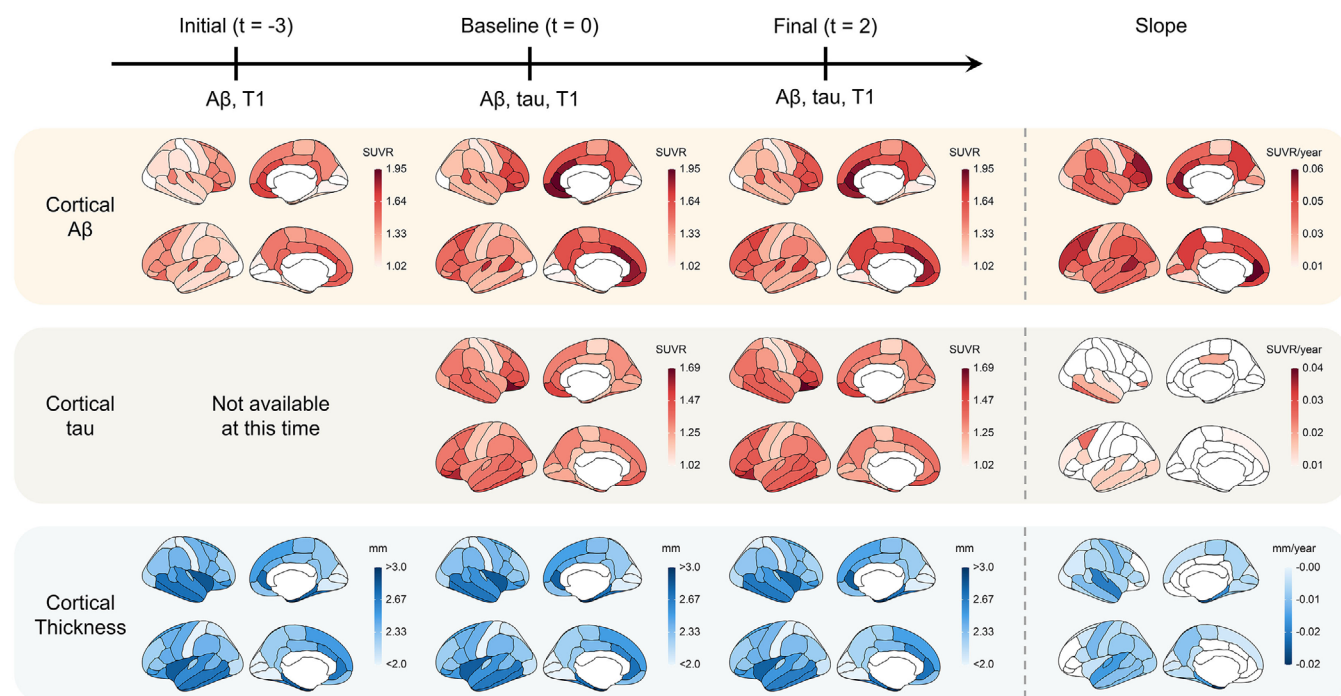


**FIGURE 1** Study design of HABS and spatiotemporal progression of A $\beta$ , tau, and cortical thickness. The baseline of HABS was defined as the time when tau-PET images were initially available ( $t = 0$ , where  $t$  indicates the time in years from baseline). Spatiotemporal progression of A $\beta$ , tau, and cortical thickness was shown in the first three columns. The mean values of each brain region at three time points were derived across participants. The brain regions with a significant increase rate of A $\beta$  and tau and significant decrease rate of cortical thickness calculated by the linear mixed model after FDR correction ( $P < 0.05$ ) and controlling covariates of age, sex, race, years of education, and apolipoprotein E  $\epsilon$ 4 status are shown in the last column. A $\beta$ , amyloid beta; FDR, false discovery rate; HABS, Harvard Aging Brain Study; PET, positron emission tomography; SUVR, standardized uptake value ratio.

and superior temporal lobe and frontal pole. There were 51 brain regions that displayed significant cortical thickness reduction, with the entorhinal cortex, temporal lobe, and parahippocampus having the fastest reductions.

### 3.3 | The correlation between the initial, slope, and final value of imaging biomarkers and cognition

Figure 2 illustrates the partial correlation between the initial value, slope, and final value of cognition of imaging summary values of A $\beta$ ,

tau, and cortical thickness after controlling for age, sex, race, years of education, and APOE  $\epsilon$ 4 status as covariates. The results were corrected using FDR ( $P < 0.05$ ). The slope of A $\beta$  had the highest correlation with the slope of tau ( $r = 0.346$ ,  $P < 0.001$ ), followed by the slope of cognition ( $r = -0.320$ ,  $P < 0.001$ ), but had no correlation with the slope of cortical thickness ( $r = -0.138$ ,  $P = 0.106$ ). The slope of tau was highly correlated with the slopes of cortical thickness ( $r = -0.350$ ,  $P < 0.001$ ) and cognition ( $r = -0.381$ ,  $P < 0.001$ ). The slope of cortical thickness had a marked correlation with the slope of cognition ( $r = 0.325$ ,  $P < 0.001$ ). The initial A $\beta$ , tau, and cortical thickness were not significantly associated with the initial values of cognition but

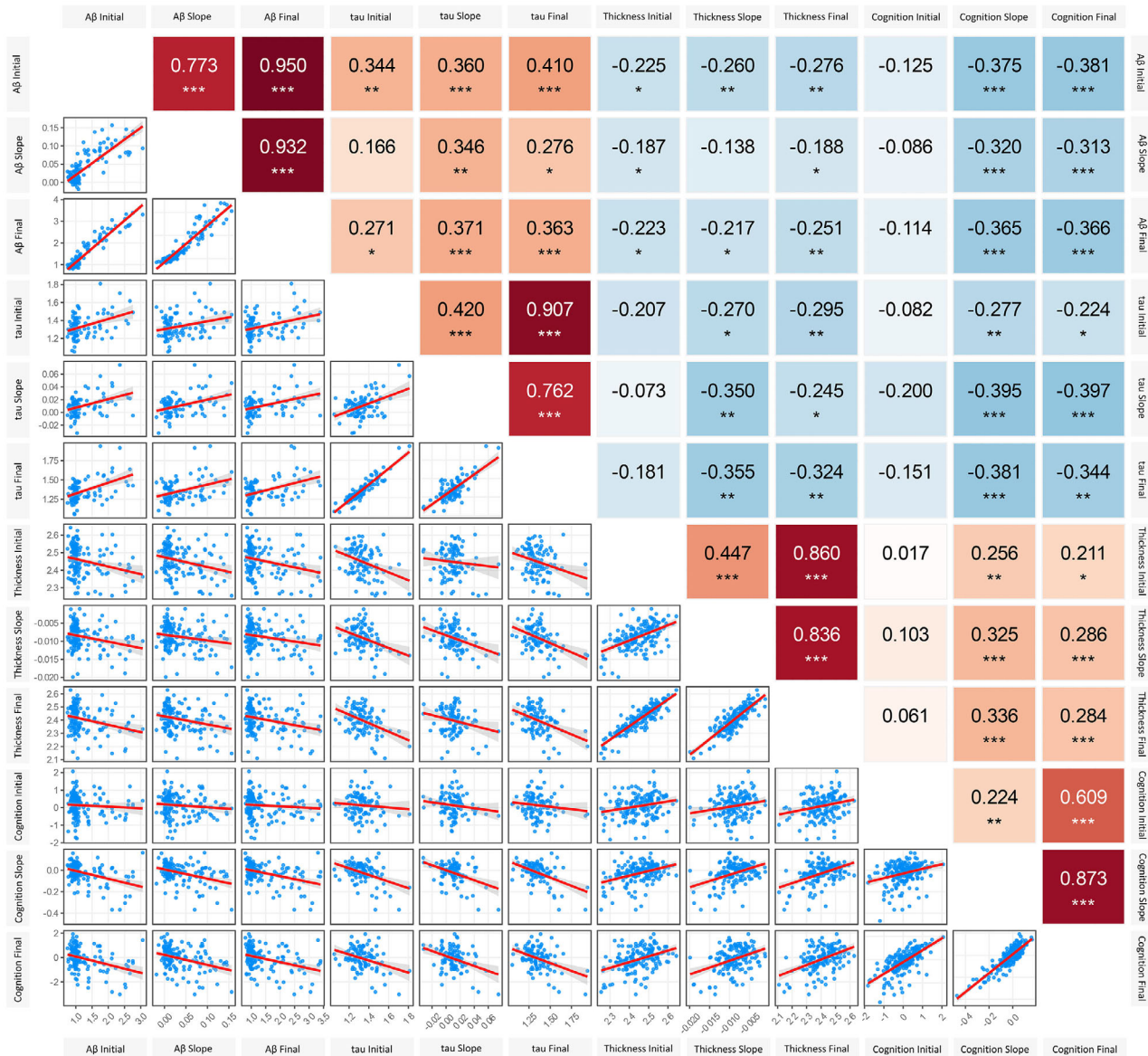


**FIGURE 2** The association pattern between the initial, slope, and final value of imaging biomarkers and cognition. The brain regions with significant change rates in amyloid beta (Aβ), tau, and cortical thickness were selected as meta-region of interest and the summary value of each kind of imaging data at different time points was calculated for each participant. The linear mixed model was used to estimate the individual slope of cognition and the summary value of imaging data. The partial correlations between the initial value, slope, and final value of cognition and imaging summary values of Aβ, tau, and cortical thickness are shown in the upper triangle after controlling for age, sex, race, years of education, and apolipoprotein E ε4 status as covariates. False discovery rate correction ( $P < 0.05$ ) for multiple comparisons was used. A series of scatter plots with fitted lines are shown in the lower triangle, where each point in the scatter plot represents one participant. (\* represents  $0.01 \leq P < 0.05$ , \*\* represents  $0.001 \leq P < 0.01$ , and \*\*\* represents  $0 \leq P < 0.001$ ).

were significantly associated with both slope and final values of cognition ( $P < 0.01$ ). These suggested that the imaging biomarkers were associated with the decline rate of cognitive function.

### 3.4 | Partial least squares structural equation modeling

PLS-SEM was used to analyze a conceptual Aβ–tau–atrophy–cognition pathway following the sequence of baseline, slope, and final value

that takes AD risk factors into account (Figure 3B). The goodness-of-fit of the model was 0.345. Aβ at baseline was positively correlated with the slope of tau ( $\beta = 0.436, P < 0.001$ ), and the slope of tau was negatively correlated with the cortical thickness ( $\beta = -0.305, P = 0.016$ ) at the final time point. The slope of Aβ was also positively correlated with tau ( $\beta = 0.418, P = 0.001$ ) at the final time point. Tau at baseline was negatively correlated with the slope of cortical thickness ( $\beta = -0.306, P = 0.004$ ), and the slope of cortical thickness was positively correlated with cognition ( $\beta = 0.288, P = 0.040$ ) at the final time point. Cortical thickness at baseline was signifi-

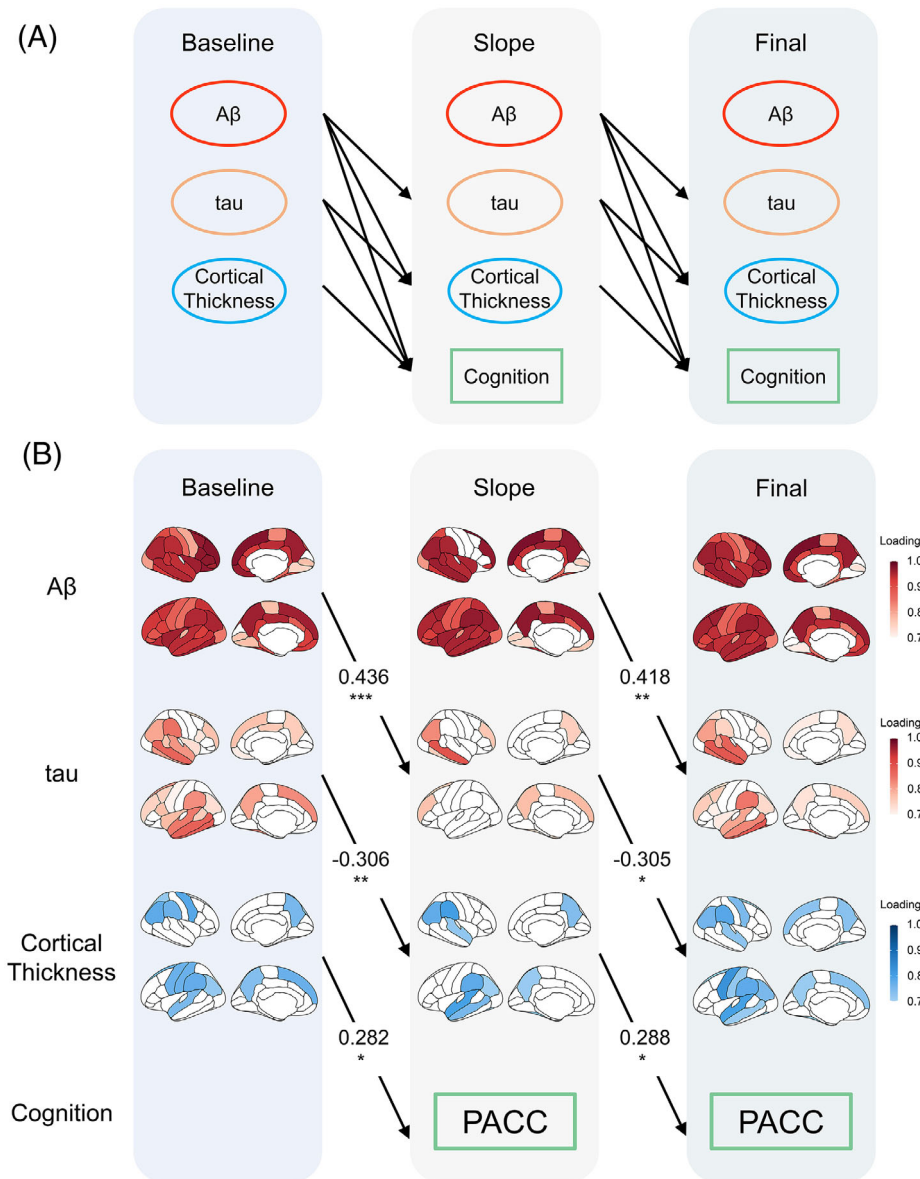


**FIGURE 3** Partial least squares structural equation model in Harvard Aging Brain Study. (A) Partial least squares structural equation modeling PLS-SEM was used to analyze a priori hypothesized amyloid beta ( $A\beta$ )-tau-atrophy-cognition pathway following the sequence of baseline, slope, final time point, and taking Alzheimer's disease risk factors (age, sex, years of education, and apolipoprotein E  $\epsilon 4$  status) into account. Ellipses represent latent variables, and rectangles represent observed variables. (B) Full frame model. Brain maps represent latent variables, and brain regions with indicator loadings greater than 0.7 were plotted. Only the paths that were statistically significant at  $P < 0.05$  after false discovery rate correction were represented and the standardized coefficients were shown.  $A\beta$  at baseline was significantly positively correlated with the slope of tau ( $\beta = 0.436$ ,  $P < 0.001$ ), and the slope of  $A\beta$  was also significantly positively correlated with tau at the final time point ( $\beta = 0.418$ ,  $P = 0.001$ ). Tau at baseline was significantly negatively correlated with the slope of cortical thickness ( $\beta = -0.306$ ,  $P = 0.004$ ), and the slope of tau was also significantly negatively correlated with cortical thickness at the final time point ( $\beta = -0.305$ ,  $P = 0.016$ ). Cortical thickness at baseline was significantly positively correlated with the slope of cognition ( $\beta = 0.282$ ,  $P = 0.040$ ), and the slope of cortical thickness was also significantly positively correlated with cognition at the final time point ( $\beta = 0.288$ ,  $P = 0.040$ ). (\* represents  $0.01 \leq P < 0.05$ , \*\* represents  $0.001 \leq P < 0.01$ , and \*\*\* represents  $0 \leq P < 0.001$ ). PACC, Preclinical Alzheimer's Cognitive Composite.

cantly positively correlated with the slope of cognition ( $\beta = 0.282$ ,  $P = 0.040$ ). Moreover, the results of the fully connected model showed that  $A\beta$ -tau-atrophy-cognition is the most significant order, which is consistent with the above conclusion. The results of this model are presented in the [Supplementary materials](#).

### 3.5 | Cross-validation in the ADNI dataset

The aforementioned results were cross-validated using the ADNI dataset. The linear mixed model was used to estimate the slopes of  $A\beta$ , tau, and cortical thickness in each brain region after controlling

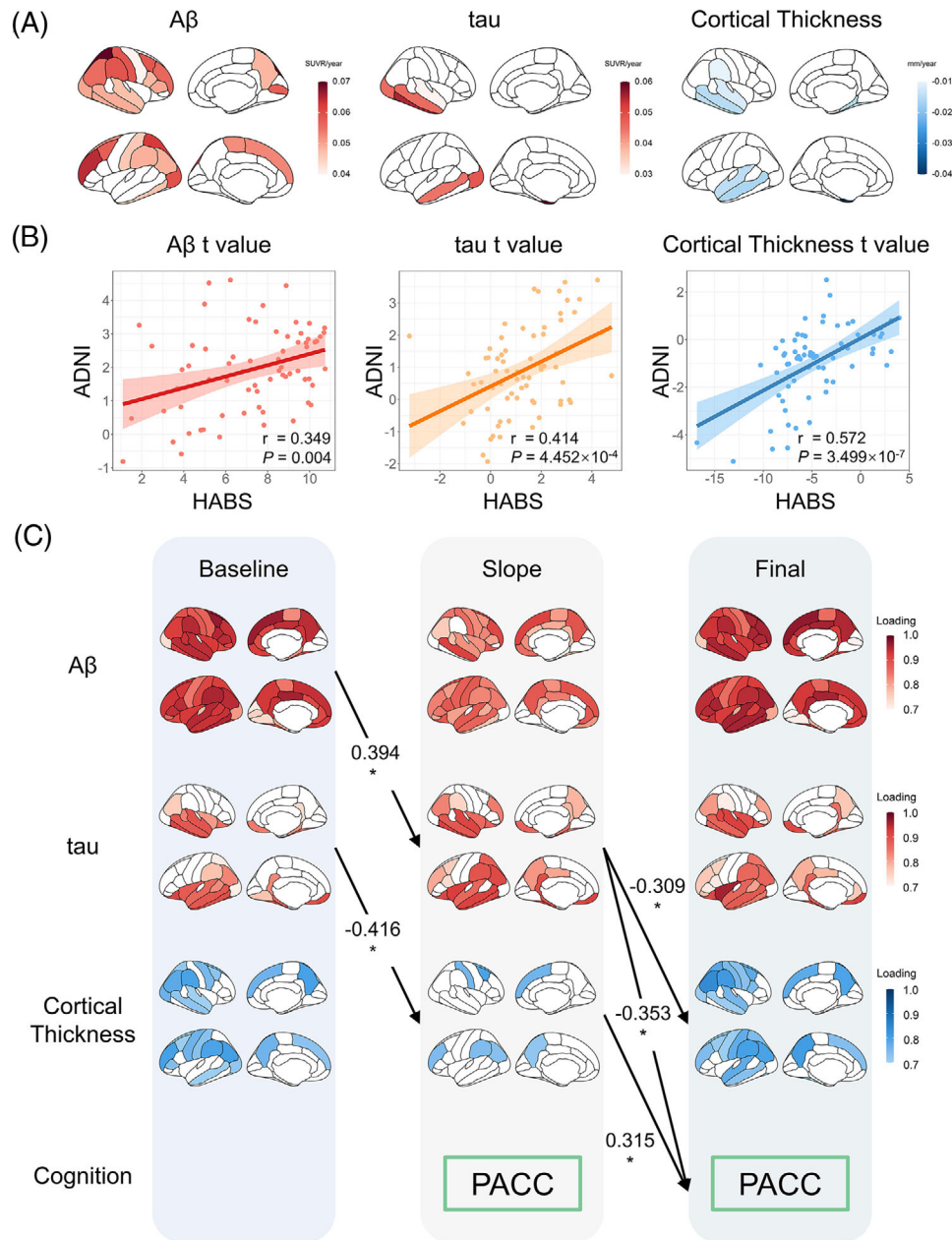


**FIGURE 4** Cross-validation in the Alzheimer's Disease Neuroimaging Initiative (ADNI) dataset. (A) The brain regions with a significant increased rate of amyloid beta ( $A\beta$ ) and tau and significant decreased rate of cortical thickness calculated by a linear mixed model after false discovery rate (FDR) correction ( $P < 0.05$ ) and controlling covariates of age, sex, race, years of education, and apolipoprotein E  $\epsilon 4$  status. (B) Correlation of  $t$  values for the slope of each brain region in the Harvard Aging Brain Study (HABS) and ADNI dataset for  $A\beta$ , tau, and cortical thickness, respectively. (C) Full frame model in the ADNI dataset. Brain maps represent latent variables, and brain regions with indicator loadings greater than 0.7 were plotted. Only the paths that were statistically significant at  $P < 0.05$  after FDR correction are represented and the standardized coefficients are shown. (\* represents  $0.01 \leq P < 0.05$ , \*\* represents  $0.001 \leq P < 0.01$  and \*\*\* represents  $0 \leq P < 0.001$ ). PACC, Preclinical Alzheimer's Cognitive Composite.

for covariates of age, sex, race, years of education, and APOE  $\epsilon 4$  status. Brain regions with  $P < 0.05$  after FDR correction are shown in Figure 4A. The  $t$  statistics of the slopes in each brain region were highly correlated between the HABS and ADNI data in  $A\beta$  ( $r = 0.349$ ,  $P = 0.004$ ), tau ( $r = 0.414$ ,  $P < 0.001$ ), and cortical thickness ( $r = 0.572$ ,  $P < 0.001$ ; Figure 4B).

PLS-SEM with the same structure was fitted in the ADNI dataset, and similar results were obtained (Figure 4C). The goodness-of-fit of the model was 0.336.  $A\beta$  at baseline was positively correlated with the slope of tau ( $\beta = 0.394$ ,  $P = 0.038$ ), and the slope of tau was negatively correlated with the final cortical thickness ( $\beta = -0.309$ ,  $P = 0.038$ ) and cognition ( $\beta = -0.353$ ,  $P = 0.038$ ). Tau at baseline was negatively

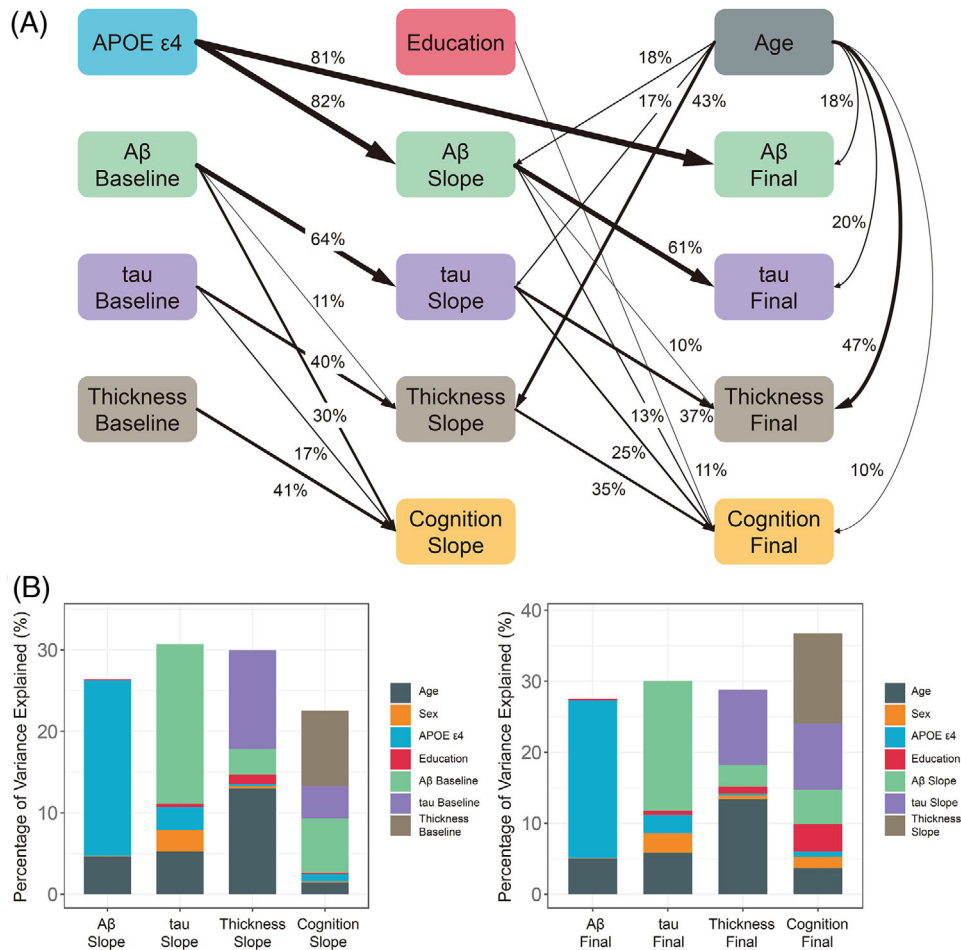


**FIGURE 5** Quantifying the proportion of variance explained by imaging biomarkers and AD risk factors. (A) The percentage of variance explained by the latent and observed variables in PLS-SEM (only variables that explain more than 10% of the variance are shown). (B) Stacked bar charts of the percentage of variance explained by imaging biomarkers and AD risk factors, respectively, for slope and final time point in PLS-SEM. Aβ, amyloid beta; AD, Alzheimer's disease; APOE, apolipoprotein E; PLS-SEM, partial least squares structural equation modeling.

correlated with the slope of cortical thickness ( $\beta = -0.416, P = 0.038$ ), and the slope of cortical thickness was positively correlated with the final cognition ( $\beta = 0.315, P = 0.038$ ).

### 3.6 | Quantifying the contribution of imaging biomarkers and AD risk factors

Figure 5 shows the percentage of variance explained by the latent and observed variables in PLS-SEM; only variables that explain more than 10% of the variance were plotted. The PLS-SEM explained 23% of the variance in the cognition slope, with baseline Aβ, tau, and cortical thickness each independently explaining 30%, 17%, and 41%, respectively, of the variance. APOE ε4 status explained 82% of the variance in the Aβ slope. Baseline Aβ and age explained 64% and 17%, respectively, of the variance in the tau slope. Age, baseline tau, and Aβ explained 43%, 40%, and 11%, respectively, of the variance in cortical thickness slope. At the final time point, the PLS-SEM explained 37% of the variance in cognition, with the slope of Aβ, tau, and cortical thickness each

independently explaining 13%, 25%, and 35%, respectively, of the variance and the AD risk factor of education and age explaining 11% and 10%, respectively, of the variance (Figure 5). Meanwhile, APOE ε4 status explained 81% of the variance in Aβ. Aβ slope and age explained 61% and 20%, respectively, of the variance in tau. Age, the slope of tau, and Aβ explained 47%, 37%, and 10% of the variance in cortical thickness, respectively.

## 4 | DISCUSSION

This study has provided strong support to the biomarker framework that is empirically grounded in the AD hypothesis. We have shown that Aβ burden at baseline is associated with the slope of tau accumulation that leads to final cortical thickness reduction, and tau accumulation at baseline is correlated with the decrease in cortical thickness that results in final cognitive decline. By assessing the dynamic trajectories of biomarkers across the AD continuum, we have also quantified the distinctive contributing proportions of AD pathology for the first time,

where the percentage of slope variance explained with the incorporation of risk factors is 26% for A $\beta$  deposition, 31% for tau accumulation, 30% for brain atrophy, and 23% for cognitive decline. More specifically, A $\beta$  burden has accounted for 64% of explained variance in tau accumulation, tau accumulation for 40% of explained variance in cortical thickness, and cortical thickness for 41% of explained variance in cognitive decline.

The A-T-N framework has integrated A $\beta$ -proteinopathy, tauopathy, and neurodegeneration into a common paradigm and is considered an evidence-based representation of the pathobiology of AD. However, critical aspects regarding the sequential order of biomarkers are lacking in this model, which is a widely acknowledged issue by researchers but has rarely been addressed. Our findings have suggested that A $\beta$  deposition preceded tau accumulation, brain atrophy, and cognitive decline, and A $\beta$  burden at baseline is associated with the change rate of tau accumulation and final tau level. This shows alignment with previous studies supporting the amyloid-cascade hypothesis, in which the initial increase in A $\beta$  burden is correlated with the tau level, and tau accumulation has increased rapidly in the subjects with high A $\beta$  burden.<sup>25,26</sup> We also tested other possible situations, and the new results supported the hypothesis of the A $\beta$ -tau-atrophy-cognition pathway. Interestingly, neither A $\beta$  burden at baseline nor the change rate of A $\beta$  deposition related to the change rate and final value of cortical thickness, whereas only tau demonstrated direct associations with cortical thickness. It indicated that A $\beta$  deposition did not directly affect the change of downstream neurodegeneration biomarkers, but tau accumulation did. Recently, it was reported that the contribution of A $\beta$  pathology to degeneration (measured by CSF neurofilament light [NfL]) was mediated by tau pathology (measured by CSF p-tau) and A $\beta$  pathology has a tau-independent role in neurodegeneration.<sup>27</sup> Both of these evidences indicated that AD biological progression may be driven in an ordinal manner (A $\rightarrow$ T $\rightarrow$ N); that is, A $\beta$  deposition caused tau accumulation, and tau accumulation resulted in the subsequent brain atrophy.<sup>3</sup>

We have further calculated the contributing proportions of A $\beta$  burden, tau accumulation, and brain atrophy at baseline to cognitive decline. A $\beta$  burden, tau accumulation, and cortical thickness at baseline accounted for 30%, 17%, and 41%, respectively, of the variance of cognitive decline. In addition, the slope of A $\beta$  burden, tau accumulation, and cortical thickness explained 13%, 25%, and 35% of the variance of the final cognition, respectively. These findings highlighted brain atrophy as the most vital contributor to cognitive decline, while the effect of A $\beta$  deposition is likely to be indirectly mediated by tau accumulation and brain atrophy in the later stages of AD progression.<sup>13,28</sup> On the other hand, the brain regions with faster rates of A $\beta$  deposition, tau accumulation, and brain atrophy have overlapped with the locations vulnerable to cognitive performance, such as the inferior, middle, and superior temporal lobe; anterior cingulate; entorhinal cortex; and the parahippocampus.

Because the imaging biomarkers may be insufficient to address the pathogenesis of AD,<sup>12,13</sup> we have taken into account the effects of AD risk factors in our models, including age, sex, APOE  $\epsilon$ 4, and education. We have found that advanced age has the strongest association with

brain atrophy compared to other features, where a great number of studies have reported its mediating effects. Similar to age, the APOE  $\epsilon$ 4 allele has been acknowledged as a critical risk factor for AD, where its propensity to undergo proteolytic cleavage generating N- and C-terminal fragments could result in A $\beta$  accumulation. We have affirmed this relationship by detecting 81% explained variance of APOE  $\epsilon$ 4 allele in increasing A $\beta$  burden. As expected, higher education levels also significantly prevented cognitive decline. The evidence has indicated that AD risk factors, along with AD pathology, promote the progression of AD biological and clinical phenotype.<sup>29,30</sup>

This study has presented several strengths. To our knowledge, the temporal sequence and spatial extent of AD biological and clinical biomarkers were the main focus in previous studies, whereas our investigation systematically demonstrated the extent to which the AD pathological events accounted for the subsequent biological and clinical progression for the first time. Second, the data consisting of different phenotypes with long-term follow-up has enabled us to assess the dynamic trajectory of biomarkers during AD progression, which has significantly augmented the scope of evidence compared to prior imaging studies. Third, the longitudinal measurements of various imaging biomarkers have allowed us to establish distinct models that serve as an explicit paradigm for testing the assumptions about the interrelationships among A $\beta$ , tau, neurodegeneration, and cognitive decline. Finally, our results have been validated in two independent cohorts, and the robustness of the findings could optimize the current research framework.

However, there are also limitations we must acknowledge. It is possible that only a restricted proportion of the variance in biological and clinical progression was accounted for by the AD pathology and AD risk factors, suggesting that other pathological conditions such as white matter lesion burden,  $\alpha$ -synuclein, TAR DNA-binding protein 43, or Lewy body pathologies also contributed to the onset and development of AD.<sup>31-34</sup> Second, because our study sample only included 360 participants primarily derived from European ancestry, whether the results are representative of the other population groups requires further validation. Third, despite that the neuroimaging protocols implemented by different cohorts have minimized the non-biological variance of biomarker measures, there remains a possibility of residual scanner variability in multisite studies and improper data harmonization. In addition, as the progression of AD could persist over a decade, the length of follow-up (5 years) in our study might restrict the generalization of our findings. However, we believe the effects of this relatively short follow-up period are minimal, given that a majority of AD imaging studies had shown similarities in terms of the follow-up period and were able to pinpoint significant pathological changes.<sup>35-37</sup> Finally, although we have attempted to unveil differential stage-related pathophysiological mechanisms by incorporating APOE  $\epsilon$ 4 into our models, further information regarding other stage-specific genetic contributions remains limited due to the dataset.

In conclusion, our study has provided vital evidence concurring with the previously proposed A $\beta$  cascade hypothesis, in which A $\beta$  burden significantly incites tau accumulation that subsequently leads to brain atrophy.<sup>38</sup> The quantification of AD pathology's contribution to

biological and clinical progression across the AD continuum has also substantiated the accurate effect of AD pathology on the disease progression and cognitive decline. Thus, treatments targeting A $\beta$  and tau should be considered, as they can partially alleviate the process of neurodegeneration and prevent cognitive decline.

#### AUTHOR CONTRIBUTIONS

Wei Cheng and Jianfeng Feng had full access to all of the data in the study and take responsibility for the integrity of the data and the accuracy of the data analysis. *Concept and design:* Wei Cheng and Jianfeng Feng. *Acquisition, analysis, or interpretation of data:* All authors. *Drafting of the manuscript:* Wei Zhang, Hui-Fu Wang, and Kevin Kuo. *Critical revision of the manuscript for important intellectual content:* Wei Zhang, Hui-Fu Wang, Kevin Kuo, Linbo Wang, Yuzhu Li, Jintai Yu, Jianfeng Feng, and Wei Cheng. *Statistical analysis:* Wei Zhang and Hui-Fu Wang. *Obtained funding:* Wei Cheng, Jianfeng Feng, Jintai Yu, and Hui-Fu Wang. All authors read and approved the final manuscript.

#### ACKNOWLEDGMENTS

ADNI data collection and sharing for this project was funded by the Alzheimer's Disease Neuroimaging Initiative (ADNI) (National Institutes of Health Grant U01 AG024904) and DOD ADNI (Department of Defense award number W81XWH-12-2-0012). ADNI is funded by the National Institute on Aging, the National Institute of Biomedical Imaging and Bioengineering, and through generous contributions from the following: AbbVie; Alzheimer's Association; Alzheimer's Drug Discovery Foundation; Araclon Biotech; BioClinica, Inc.; Biogen; Bristol-Myers Squibb Company; CereSpir, Inc.; Cogstate; Eisai Inc.; Elan Pharmaceuticals, Inc.; Eli Lilly and Company; EuroImmun; F. Hoffmann-La Roche Ltd and its affiliated company Genentech, Inc.; Fujirebio; GE Healthcare; IXICO Ltd.; Janssen Alzheimer Immunotherapy Research & Development, LLC; Johnson & Johnson Pharmaceutical Research & Development LLC; Lumosity; Lundbeck; Merck & Co., Inc.; Meso Scale Diagnostics, LLC; NeuroRx Research; Neurotrack Technologies; Novartis Pharmaceuticals Corporation; Pfizer Inc.; Piramal Imaging; Servier; Takeda Pharmaceutical Company; and Transition Therapeutics. The Canadian Institutes of Health Research is providing funds to support ADNI clinical sites in Canada. Private sector contributions are facilitated by the Foundation for the National Institutes of Health ([www.fnih.org](http://www.fnih.org)). The grantee organization is the Northern California Institute for Research and Education, and the study is coordinated by the Alzheimer's Therapeutic Research Institute at the University of Southern California. ADNI data are disseminated by the Laboratory for Neuro Imaging at the University of Southern California. The authors thank all the researchers and participants in the ADNI initiative. As such, the investigators within the ADNI contributed to the design and implementation of ADNI and/or provided data but did not participate in analysis or writing of this report. A complete listing of ADNI investigators can be found at: [http://adni.loni.usc.edu/wp-content/uploads/how\\_to\\_apply/ADNI\\_Acknowledgement\\_List.pdf](http://adni.loni.usc.edu/wp-content/uploads/how_to_apply/ADNI_Acknowledgement_List.pdf). This study was supported by grants from the National Natural Science Foundation of China (No. 82071997), the Shanghai Rising-Star Program (No. 21QA1408700), the National Key R&D Program of China (No.

2019YFA0709502, No. 2018YFC1312904), the Shanghai Municipal Science and Technology Major Project (No. 2018SHZDZX01), the 111 Project (No. B18015), the Science and Technology Innovation 2030 Major Projects (2022ZD0211600), the National Natural Science Foundation of China (82071201), the Shanghai Municipal Health Commission New interdisciplinary research project (2022JC014), the STI2030-Major Projects (2022ZD0211600) and the Taishan Scholars Program of Shandong Province (tsqn201812157). The funding sources had no role in the design and conduct of the study; collection, management, analysis, and interpretation of the data; preparation, review, or approval of the manuscript; and decision to submit the manuscript for publication.

#### CONFLICTS OF INTEREST

The authors declare no competing interests. Author disclosures are available in the [supporting information](#).

#### REFERENCES

1. Frisoni GB, Altomare D, Thal DR, et al. The probabilistic model of Alzheimer disease: the amyloid hypothesis revised. *Nat Rev Neurosci*. 2022;23:53-66.
2. Wang HF, Shen XN, Li JQ, et al. Clinical and biomarker trajectories in sporadic Alzheimer's disease: a longitudinal study. *Alzheimers Dement (Amst)*. 2020;12:e12095.
3. Jack CR Jr, Bennett DA, Blennow K, et al. NIA-AA Research Framework: toward a biological definition of Alzheimer's disease. *Alzheimers Dement*. 2018;14:535-562.
4. Yu JT, Li JQ, Suckling J, et al. Frequency and longitudinal clinical outcomes of Alzheimer's AT(N) biomarker profiles: a longitudinal study. *Alzheimers Dement*. 2019;15:1208-1217.
5. Boyle PA, Yu L, Wilson RS, Leurgans SE, Schneider JA, Bennett DA. Person-specific contribution of neuropathologies to cognitive loss in old age. *Ann Neurol*. 2018;83:74-83.
6. Jack CR Jr, Wiste HJ, Therneau TM, et al. Associations of amyloid, tau, and neurodegeneration biomarker profiles with rates of memory decline among individuals without dementia. *JAMA*. 2019;321:2316-2325.
7. Planche V, Villain N. US Food and Drug Administration approval of aducanumab-is amyloid load a valid surrogate end point for Alzheimer disease clinical trials? *JAMA Neurol*. 2021;78:1307-1308.
8. Rubin R. Recently approved alzheimer drug raises questions that might never be answered. *JAMA*. 2021;326:469-472.
9. Dunn B, Stein P, Cavazzoni P. Approval of aducanumab for Alzheimer disease-the FDA's perspective. *JAMA Intern Med*. 2021;181:1276-1278.
10. Honig LS, Vellas B, Woodward M, et al. Trial of solanezumab for mild dementia due to Alzheimer's disease. *N Engl J Med*. 2018;378:321-330.
11. Budd Haeberlein S, O'Gorman J, Chiao P, et al. Clinical development of aducanumab, an anti-A $\beta$  human monoclonal antibody being investigated for the treatment of early Alzheimer's disease. *J Prev Alzheimers Dis*. 2017;4:255-263.
12. Boyle PA, Wang T, Yu L, et al. To what degree is late life cognitive decline driven by age-related neuropathologies? *Brain*. 2021;144:2166-2175.
13. Tosun D, Demir Z, Veitch DP, et al. Contribution of Alzheimer's biomarkers and risk factors to cognitive impairment and decline across the Alzheimer's disease continuum. *Alzheimers Dement*. 2022;18:1370-1382.
14. Dagley A, LaPoint M, Huijbers W, et al. Harvard Aging Brain Study: dataset and accessibility. *Neuroimage*. 2017;144:255-258.

15. Weiner MW, Veitch DP, Aisen PS, et al. The Alzheimer's Disease Neuroimaging Initiative: a review of papers published since its inception. *Alzheimers Dement*. 2013;9:e111-94.
16. Donohue MC, Sperling RA, Salmon DP, et al. The Preclinical Alzheimer Cognitive Composite measuring amyloid-related decline. *JAMA Neurol*. 2014;71:961-970.
17. Papp KV, Rentz DM, Orlovsky I, Sperling RA, Mormino EC. Optimizing the preclinical Alzheimer's cognitive composite with semantic processing: the PACC5. *Alzheimers Dement (N Y)*. 2017;3:668-677.
18. Buckley RF, Mormino EC, Amariglio RE, et al. Sex, amyloid, and APOE epsilon 4 and risk of cognitive decline in preclinical Alzheimer's disease: findings from three well-characterized cohorts. *Alzheimers Dement*. 2018;14:1193-1203.
19. Fischl B, Salat DH, Busa E, et al. Whole brain segmentation: automated labeling of neuroanatomical structures in the human brain. *Neuron*. 2002;33:341-355.
20. Greve DN, Svarer C, Fisher PM, et al. Cortical surface-based analysis reduces bias and variance in kinetic modeling of brain PET data. *Neuroimage*. 2014;92:225-236.
21. Greve DN, Salat DH, Bowen SL, et al. Different partial volume correction methods lead to different conclusions: an F-18-FDG-PET study of aging. *Neuroimage*. 2016;132:334-343.
22. Rousset OG, Ma YL, Evans AC. Correction for partial volume effects in PET: principle and validation. *J Nucl Med*. 1998;39:904-911.
23. Benjamini Y, Hochberg Y. Controlling the false discovery rate: a practical and powerful approach to multiple testing. *J R Stat Soc Series B Stat Methodol*. 1995;57:289-300.
24. Hair JF, Risher JJ, Sarstedt M, Ringle CM. When to use and how to report the results of PLS-SEM. *Eur Bus Rev*. 2019;31:2-24.
25. Hanseeuw BJ, Betensky RA, Jacobs HIL, et al. Association of amyloid and tau with cognition in preclinical Alzheimer disease: a longitudinal study. *JAMA Neurol*. 2019;76:915-924.
26. Jack CR Jr, Wiste HJ, Schwarz CG, et al. Longitudinal tau PET in ageing and Alzheimer's disease. *Brain*. 2018;141:1517-1528.
27. Salvadó G, Milà-Alomà M, Shekari M, et al. Cerebral amyloid- $\beta$  load is associated with neurodegeneration and gliosis: mediation by p-tau and interactions with risk factors early in the Alzheimer's continuum. *Alzheimers Dement*. 2021;17:788-800.
28. Bejanin A, Schonhaut DR, La Joie R, et al. Tau pathology and neurodegeneration contribute to cognitive impairment in Alzheimer's disease. *Brain*. 2017;140:3286-3300.
29. Yu JT, Xu W, Tan CC, et al. Evidence-based prevention of Alzheimer's disease: systematic review and meta-analysis of 243 observational prospective studies and 153 randomised controlled trials. *J Neurol Neurosurg Psychiatry*. 2020;91:1201-1209.
30. Jia L, Quan M, Fu Y, et al. Dementia in China: epidemiology, clinical management, and research advances. *Lancet Neurol*. 2020;19:81-92.
31. Rabin JS, Schultz AP, Hedden T, et al. Interactive associations of vascular risk and  $\beta$ -Amyloid burden with cognitive decline in clinically normal elderly individuals: findings from the Harvard Aging Brain Study. *JAMA Neurol*. 2018;75:1124-1131.
32. Yang HS, Yu L, White CC, et al. Evaluation of TDP-43 proteinopathy and hippocampal sclerosis in relation to APOE  $\epsilon$ 4 haplotype status: a community-based cohort study. *Lancet Neurol*. 2018;17:773-781.
33. Goedert M. NEURODEGENERATION. Alzheimer's and Parkinson's diseases: the prion concept in relation to assembled A $\beta$ , tau, and  $\alpha$ -synuclein. *Science*. 2015;349:1255555.
34. Dawe RJ, Yu L, Arfanakis K, Schneider JA, Bennett DA, Boyle PA. Late-life cognitive decline is associated with hippocampal volume, above and beyond its associations with traditional neuropathologic indices. *Alzheimers Dement*. 2020;16:209-218.
35. Rauchmann B-S, Ghaseminejad F, Mekala S, Pernecky R, Alzheimers Dis Neuroimaging I. Cerebral microhemorrhage at MRI in mild cognitive impairment and early Alzheimer disease: association with tau and amyloid beta at PET imaging. *Radiology*. 2020;296:134-142.
36. Ozlen H, Binette AP, Kobe T, et al. Spatial extent of amyloid-beta levels and associations with tau-PET and cognition. *JAMA Neurol*. 2022;79:1025-1035.
37. Strikwerda-Brown C, Hobbs DA, Gonneaud J, et al. Association of elevated amyloid and tau positron emission tomography signal with near-term development of Alzheimer disease symptoms in older adults without cognitive impairment. *JAMA Neurol*. 2022;79:975-985.
38. Guo T, Korman D, Baker SL, Landau SM, Jagust WJ. Longitudinal cognitive and biomarker measurements support a unidirectional pathway in Alzheimer's disease pathophysiology. *Biol Psychiatry*. 2021;89:786-794.

## SUPPORTING INFORMATION

Additional supporting information can be found online in the Supporting Information section at the end of this article.

**How to cite this article:** Zhang W, Wang H-F, Kuo K, et al. Contribution of Alzheimer's disease pathology to biological and clinical progression: A longitudinal study across two cohorts. *Alzheimer's Dement*. 2023;1-11. <https://doi.org/10.1002/alz.12992>